Planet. Space Sci., Vol. 38, No. 11, pp. 1399–1408, 1990
Printed in Great Britain.

0032–0633/90 $3.00+0.00
Pergamon Press plc

A VIBRATIONAL ANALYSIS OF THE O_2 $(A^3\Sigma_u^+)$ HERZBERG I SYSTEM USING ROCKET DATA

DAVID E. SISKIND and WILLIAM E. SHARP
Space Physics Research Laboratory, University of Michigan, Ann Arbor, MI 48109, U.S.A.

(*Received* 4 *May* 1990)

Abstract—An observation of the u.v. nightglow between 2670 and 3040 Å was conducted over White Sands Missile Range on 22 October 1984. A 1/4 m spectrometer operating at 3.5 Å resolution viewed the Earth's limb at tangent heights between 90 and 110 km for 120 s. A total of 41 spectral scans of the nightglow were obtained with the brightest feature being the O_2 $(A^3\Sigma_u^+ - X^3\Sigma_g^-)$ Herzberg I bands. The data were sorted into two groups, one from the top side of the layer and one containing the emission peak, and compared with synthetic spectra. The deduced O_2 $(A^3\Sigma_u^+)$ vibrational distributions indicate that at low altitudes, the higher vibrational levels ($v' > 6$) were relatively depleted; however, the magnitude of the vibrational shift is much less than that predicted from theories of vibrational relaxation. It is shown that increasing the electronic quenching of O_2 $(A^3\Sigma_u^+)$ with respect to the vibrational quenching can reduce the vibrational shift in the model and qualitatively explain the observations; however, several details of the vibrational distribution are not well reproduced.

INTRODUCTION

The near and middle ultraviolet nightglow result from the energy released when atomic oxygen recombines into molecular oxygen at lower thermospheric altitudes (90–110 km). Early work (Dufay, 1941; Broida and Gaydon, 1954; Chamberlain, 1955; Hennes, 1966) showed that the dominant feature in the u.v. nightglow was the O_2 $(A^3\Sigma_u^+ - X^3\Sigma_g^-)$ Herzberg I system. Later studies demonstrated that emissions from the O_2 $(A'^3\Delta_u - a^1\Delta_g)$ Chamberlain (Chamberlain, 1958), Herzberg II $(c^1\Sigma_u^- - X^3\Sigma_g^-)$ (Slanger and Huestis, 1981, 1983), and possibly Herzberg III $(A'^3\Delta_u - X^3\Sigma_g^-)$ (Sharp and Siskind, 1989) systems are also present, but with lower intensities. Note that the upper states associated with these transitions are all metastable. As Slanger and Cosby (1988) have recently commented, this metastability has hindered the laboratory study of the O_2 molecular structure. Conversely, the presence of these emissions in the nightglow means that analysis of the nightglow can be an excellent way to study the physical chemistry of metastable O_2.

One of the pioneering studies of the O_2 nightglow was that of Degen (1969). He was the first to conclusively demonstrate that the Herzberg I emission in the nightglow is characterized by a non-Boltzmann vibrational distribution. Both Degen's work, as well as later studies (Stegman and Murtagh, 1988; Sharp and Siskind, 1989) showed that typical vibrational populations peak in the range of $v' = 4$–6. In 1972, Degen proposed a model for the excitation of the Herzberg I system which assumed that the $A^3\Sigma_u^+$ state was produced by direct three-body recombination into a high vibrational level (> 10) followed by stepwise vibrational deactivation (Degen, 1972). By explicitly considering the anharmonicity of the A-state potential using the so-called SSH theory (Schwartz and Herzfeld, 1954), he calculated vibrational deactivation coefficients which increased with v' in a nonlinear fashion. By doing so, he was able to model the Herzberg I vibrational population, as seen both in the laboratory as well as in the airglow.

McDade *et al.* (1982) then extended Degen's model to consider the implications it would have on the altitude profile of individual Herzberg bands. They found that the change in atmospheric density with altitude would necessarily cause the vibrational deactivation rate (which depends upon collisions with O_2 and N_2) to decrease with increasing altitude. As a result, the vibrational distribution should be more relaxed (colder) at lower altitudes due to the increased deactivation. They discussed how this could be detected by a measurement of the Herzberg I altitude profile using two photometers, one sensitive to short wavelengths (predominantly high vibrational levels) and the other sensitive to long wavelengths (predominantly low vibrational levels). Their prediction was that the profile measured by the short wavelength photometer would peak at a higher altitude than the long wavelength photometer, as a result of the reduced deactivation at higher altitudes.

An experimental test of this prediction was conducted by Murtagh *et al.* (1986) as part of the multirocket campaign known by the acronym ETON

(Energy Transfer in the Oxygen Nightglow) (Greer *et al.*, 1986). Unfortunately, the results were negative. The profiles obtained by short and long wavelength photometers appeared largely indistinguishable or even slightly inverted (long wavelength peaking higher). Similar results were obtained in an analogous experiment by Kita *et al.* (1988). These results cast doubt on the theory of production of O_2 ($A^3\Sigma_u^+$) by direct recombination unless, as McDade and Llewellyn (1986) and Murtagh *et al.* (1986) have suggested, rapid electronic quenching was "freezing out" the vibrational distribution making it invariant with altitude. Rapid electronic quenching of the Herzberg bands had been proposed earlier by Thomas (1981), but would conflict with the low quenching rate measured in the laboratory by Kenner and Ogryzlo (1984, 1983, 1980).

One limitation of the above-described studies was their reliance upon relatively wide-band (>100 Å) photometers. While this enhances the total signal, it makes it difficult to deduce vibrational distributions or to subtract contaminating emissions. A better approach would be to measure isolated vibrational levels. In this paper, we attempt to do that by analyzing spectra of the u.v. nightglow obtained from a limb scanning spectrometer. By searching for an altitude variation in the spectra, we will be able to better quantify the effects of vibrational relaxation on the Herzberg I emission.

DATA ANALYSIS

The data to be discussed in this paper were obtained as part of a sounding rocket experiment launched from White Sands Missile Range. The flight occurred on 22 October 1984 just after midnight when the solar zenith angle was 154°. The complement of instruments included two resonance lamp modules for measuring atomic oxygen and hydrogen, photometers to measure the emission from the NO_2 continuum, the OH (9, 3) band, and O_2 (0, 0) atmospheric band, and a 1/4 m u.v. scanning spectrometer operating at 3.5 Å resolution. An analysis of the photometer observations will be reported elsewhere; here, we only discuss the measurements of the Herzberg I emission by the scanning spectrometer. The wavelength interval scanned by the digital drive of the spectrometer was 2670–3040 Å. The spectrometer was calibrated in the laboratory with an NBS calibrated tungsten lamp. Prior to taking the payload to the launcher, the spectrometer viewed a hollow cathode platinum discharge for the purpose of assigning wavelengths to the data bins. This calibration resulted in the wavelength position of the scan being accurate to within one grating step (±1.75 Å). The field of view of the telescope was measured to be 0.5 by 5.0 degrees.

The spectrometer observed the nightglow in a limb scanning geometry. This was accomplished by pointing the payload North at a zenith angle of 97° for 120 s, centered on apogee. Since the optical axis of the instrument was aligned along the payload roll axis, the field of view for a 90 km tangent height was near 41° N latitude (about Boulder, Colorado). While the rocket ascended and descended about apogee, the tangent height changed from 90 to 110 km and 41 spectral scans of the middle u.v. nightglow were thus obtained.

A preliminary analysis of these spectra was presented by Sharp and Siskind (1989). That paper discussed the fit to the various spectral features, including the Herzberg I, II and III bands, the N_2 VK bands $O(^1S)$ and Mg 2852 Å. Here, we are interested in looking at possible variations of the spectrum with altitude. Figure 1 presents a limb profile of the Herzberg I emission, showing both the individual data points and a smooth cubic spline fit. This curve was obtained by integrating the total spectra over wavelength [except for the region near the 2972 Å $O(^1S)$ line], multiplying by the fraction of emission in the spectra due to the Herzberg I emission (79%) and dividing by the fraction of the total Herzberg I emission contained in the bandpass of the spectrometer (about 40%). It should be noted that the vibrational models described below suggest that this second number may be altitude dependent and may vary from 35% at the lower altitudes (where the spectrum is shifted to lower v') to 50% at the higher altitudes. Our use of a fixed value thus introduces a possible uncertainty that could be as much as 20% at 110 km [which is not reflected in the error bars given in the Sharp and Siskind (1989) report]. In addition, we obtained an estimate of the dark count from data obtained before the nose cone ejected and subtracted this from the integrated spectra. Due to the relatively low count rates, it was not possible to obtain altitude profiles of individual vibrational levels. Instead, the 41 spectra were binned into one of two categories: high altitudes and low altitudes. Thus, as indicated by the figure, the seven low altitude scans were averaged together to produce a representative low altitude spectrum. The 34 high altitude scans were similarly averaged. The division of the profile in this fashion was motivated by the desire to yield equal counting statistics in the resulting composite scans.

Figure 1b shows the volume emission rate profile which results from an "onion peel" inversion of the slant column intensity. This shows more clearly that the spectrum which we have labelled "low" is representative of the peak of the airglow layer, while the

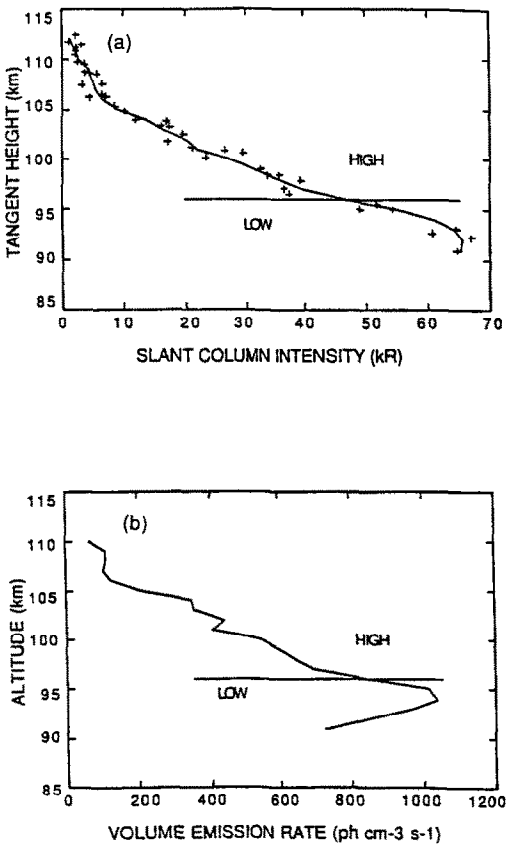

FIG. 1. LIMB PROFILE OF HERZBERG I EMISSION OBTAINED BY SCANNING SPECTROMETER ON NASA FLIGHT 33.047. (a) The solid line is a cubic spline fit to the individual data points. The horizontal line indicates the division of the profile into high and low altitude bins for subsequent spectroscopic analysis. (b) Volume emission rate corresponding to the intensity profile in (a). The high and low altitude bins are also indicated.

high altitude spectrum represents the topside of the layer.

The altitude scale in Figs 1a and b deserves some additional comment. The rocket viewed the limb when it was at altitudes between 120 and 150 km. For these rocket altitudes, the distance to the tangent point on the limb is approx. 1000 km and a one degree error in pointing translates into a 10 km error on the limb. In fact, the ACS on the payload is only accurate to within two degrees. As a result, there is a considerable uncertainty in the altitude scale in these figures. While it is clear that we are observing most of a well-defined airglow layer, we cannot place the altitude of the layer on an absolute scale. In addition, recent evidence from *Space Shuttle* observations (Swenson *et al.*, 1989) suggests that the height of the airglow layer can vary by up to 8 km along an orbital track. Indeed, our 7620 Å atmospheric band observation indicates a 3 km variation between the upleg and downleg of the rocket flight. On the other hand, it has been shown that the atmospheric band peaks about 2 km lower than the Herzberg bands (e.g. Greer *et al.*, 1986). On our flight, an average of the upleg and downleg atmospheric band profiles produced a peak at 92 km; we therefore placed the Herzberg peak at 94 km. Of course, this still leaves some uncertainty which will be discussed further below; however, to the extent that our conclusions are independent of the assumed shape of the O_2 ($A^3\Sigma_u^+$) production profile, they will be less affected by the uncertainty in the altitude profile in Fig. 1.

Figures 2a and b show the composite high and low altitude spectra as well as the fit from the synthetic calculation. While in general both spectra contain the same features, closer inspection reveals some differences. For example, the (7, 2) band at 2732 Å appears to be enhanced relative to the (6, 2) band at 2773 Å in the high altitude plot. In addition, a number of the features appear to change shape from one spectrum to another. To get a quantitative understanding of the possible differences between the two spectra, synthetic spectra were calculated and fit to each spectrum. Our fitting approach was slightly different from the technique that we have described previously (Sharp and Siskind, 1989). In that paper, we constrained the distributions of the Herzberg II and III to follow a smooth bell-shaped curve. For this paper, we have decided to loosen that constraint to allow for any fitting coefficient that was non-negative. This is for two reasons. First, recent airglow observations reported by Stegman *et al.* (1988, 1989) consistently show deviations from a smooth curve. Second, the fit to the data at high and low altitudes is better if we freely vary each vibrational level of the $c^1\Sigma_u$ and $A'^3\Delta_u$ states in an independent fashion. This may reflect real changes in these distributions or it may simply reflect the poorer counting statistics associated with dividing the composite spectrum of Sharp and Siskind (1989) into two halves. In any event, the fit to the weaker emission features is the largest uncertainty in our analysis of the spectrum and is probably the cause of the many small discrepancies seen in the curves in Figs 2a and b. On the other hand, the only noticeable difference in the deduced $A^3\Sigma_u^+$ vibrational populations between this work and our earlier paper is that we now give a slightly smaller estimate for the $v' = 4$ population (due to an overlap with $v' = 8$ bands of the Herzberg II system). The resulting A-state vibrational

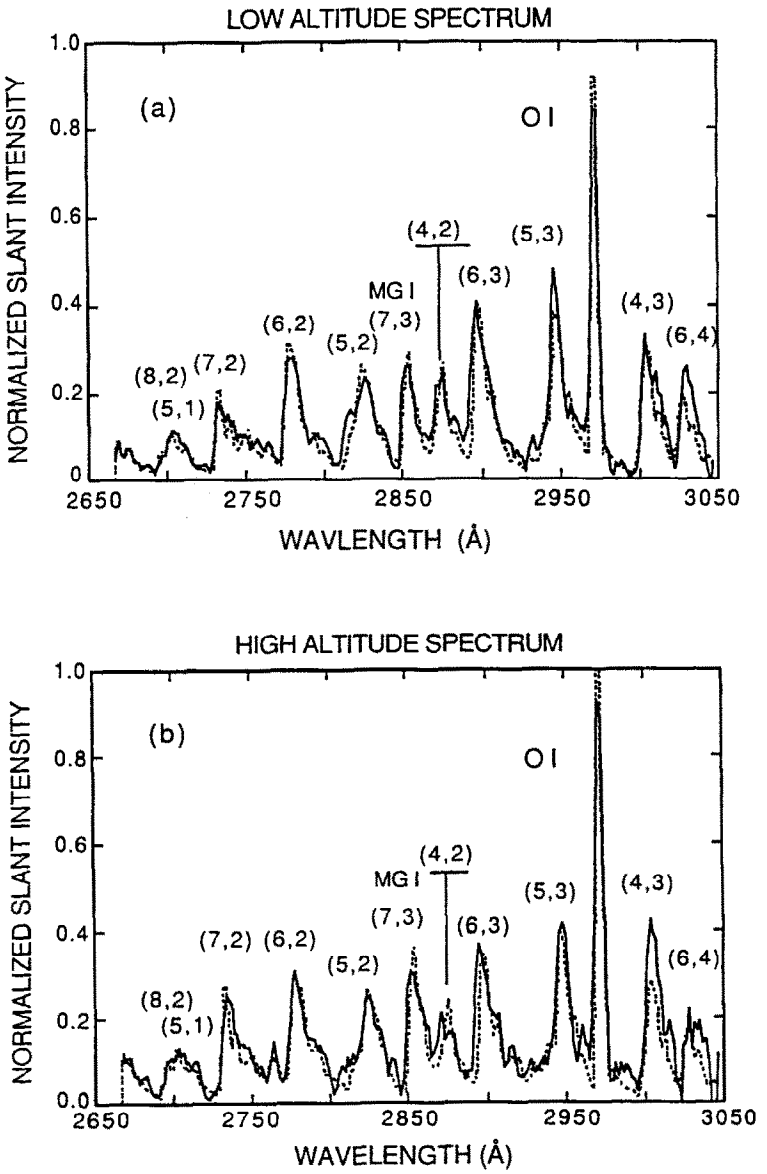

FIG. 2. SPECTRA OBTAINED FROM FLIGHT 33.047 FOR (a) LOW ALTITUDE AND (b) HIGH ALTITUDE. The definition of "high" and "low" is shown in Fig. 1. The dotted line in each panel is the calculated synthetic spectrum.

populations corresponding to Figs 2a and b are given in Fig. 3.

Figure 3 shows that there is a shift in the vibrational population of the $A^3\Sigma_u^+$ state from high to low altitudes. Specifically, the $v' = 7$, 8 and 9 levels are all depleted relative to $v' = 6$ at low altitudes. In order to understand this more clearly, Fig. 4 presents an expanded view of the data from 2670 to 2850 Å. In this figure, the high altitude spectrum (solid line) is directly compared with the low altitude spectrum (dotted line). Emission from a total of 17 bands is indicated. By normalizing the two spectra at the peak of the Herzberg I (6, 2) band at 2773 Å, we can see that the intensity is reduced in the low altitude spectra

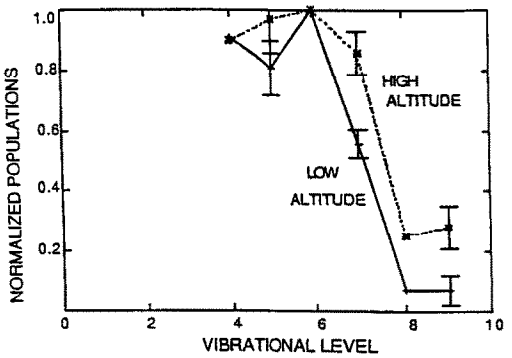

FIG. 3. DEDUCED VIBRATIONAL DISTRIBUTIONS FROM THE FIT TO THE SPECTRA SHOWN IN FIGS 2a AND b.

for wavelengths short of 2750 Å. The spectrum here is dominated by the Herzberg (7, 2), (8, 2), (9, 2) bands. Of these three, the (7, 2) is the brightest and is relatively uncontaminated by other features. The error bar that is shown at the peak of the (7, 2) band represents the one standard deviation uncertainty (about 17%) for that single wavelength bin due to the counting statistics. The error in the fit to the entire band is much less since it includes the signal from 4 to 5 wavelength bins. As a result, the change in intensity in this band at lower altitudes is statistically significant to about two standard deviation units and this is reflected in the error bars given in Fig. 3. In the case of the (8, 2) and (9, 2) bands, the statistics are poorer, there is greater contamination from weaker Herzberg II and III features and the error bars are proportionally larger (although the increased sensitivity of the detector at the shorter wavelengths partially compensates for this). While the fit to these bands at high and low altitudes remains statistically significant, it is at a lower confidence level (about 1 standard deviation unit, as shown in Fig. 3).

For vibrational levels less than six, the error bars in the fit overlap and we cannot make a conclusive statement about any altitude variation in these levels. We do note, however, that a depletion in the Herzberg I $v' = 5$ emission seen in the low altitude curve in Fig. 4 qualitatively appears similar to that reported by Stegman *et al.* (1989) from ground-based observations. There is also some evidence in Figs 2 and 4 for an altitude variation in some of the other features in the spectrum. For example, the N_2 VK (0, 6) band at 2760 Å is clearly enhanced in the high altitude

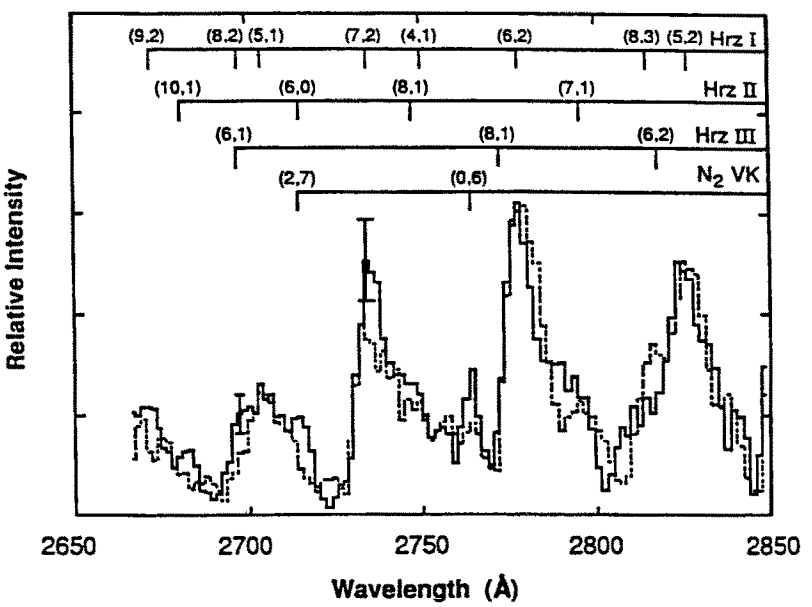

FIG. 4. EXPANDED VIEW OF THE DATA FROM 2670 TO 2850 Å.
The high altitude data (solid line) are directed compared with the low altitude data (dotted line). The two spectra have been normalized at the peak of the (6, 2) band at 2775 Å in order to highlight the changes in the spectra which occur at shorter wavelengths, in particular the reduced intensity of the (7, 2) band at 2730 Å. The location of 17 spectral features is indicated.

spectrum. In addition, some of the Herzberg II bands [e.g. the (7, 1) and (7,2) at 2788 and 2912 Å, respectively] seem to be more prominent in the high altitude data. Such variations could be of great importance, since the production of the 5577 Å green line from a $c^1\Sigma_u^-$ precursor may depend upon altitude variations of individual $c^1\Sigma_u^+$ vibrational levels (McDade *et al.*, 1984). Unfortunately, as we have already noted, the low intensities of the Herzberg II bands preclude a fit to individual $c^1\Sigma_u^-$ levels. In the discussion which follows, we will therefore concentrate on modelling the Herzberg I bands and comparing our results with the applications of the SSH model by Degen (1972) and McDade *et al.* (1982) to the Herzberg $A^3\Sigma_u^+$ state.

MODELLING

The model that we used to calculate the vibrational distribution of the $A_3\Sigma_u^+$ state was first proposed by Degen (1972). His theory was extended by McDade *et al.* (1982) to evaluate the possibility that the *A*-state vibrational distribution could be altitude dependent. Most recently, this theory has been compared with photometric observations of the Herzberg I nightglow by Murtagh *et al.* (1986) and Kita *et al.* (1988). Since our application of the theory is the same as the latter three studies cited above, only the salient features will be summarized here.

Degen (1972) proposed that the $A^3\Sigma_u^+$ state is formed by direct three-body recombination of atomic oxygen in a high lying vibrational level ($v' > 10$). The lower vibrational levels are populated by a single step ($\Delta v = 1$) vibrational relaxation process. Two loss mechanisms which can terminate this process are collisional quenching or radiative transitions to the electronic ground state. In steady-state, the population of a given vibrational level, v, can be written in terms of the population of the $(v+1)$ level as follows

$$N_v = \frac{k_{v+1,v}[M_v]N_{v+1}}{k_{v,v-1}[M_v]+k_E[M_E]+A(v)}, \quad (1)$$

where $k_{v+1,v}$ is the rate coefficient for vibrational deactivation from the $(v+1)$th to the vth level by a species M_v, k_E is the electronic quenching coefficient by a species M_E, and $A(v)$ is the radiative transition probability. In practice, the calculation begins at the highest vibrational level where the only source is the direct three-body production, and then proceeds down each individual vibrational level. For $v' = 0$, $k_{v,v-1}$ is zero and the only losses are electronic quenching and spontaneous emission.

Uncertainty surrounds all of the loss processes given in the denominator of equation (1). Of the three, the radiative transition probability, $A(v)$, is perhaps the best known. The recent tabulation by Bates (1989) gives values which average near 11 s^{-1} although, as he notes, this may be too high by a factor of 1.67. Concerning the electronic quenching coefficient, k_E, published values disagree by almost three orders of magnitude. From laboratory studies, Kenner and Ogryzlo (1980, 1983) report values in the range 1.3–2.9×10^{-13} cm^3 s^{-1} for quenching the $v' = 1$–4 levels by O_2 while Slanger *et al.* (1984) reported a value of 8×10^{-11} cm^3 s^{-1} for $v' = 8$. Quenching rates have also been estimated from rocket profiles (Murtagh *et al.*, 1986; Thomas, 1981). The numbers in these cases lie in between the laboratory values, i.e. 5–9 $\times$ 10^{-12} cm^3 s^{-1}.

Table 1. Summary of Herzberg I quenching models

	k_{10}	k_{O_2}
Model 1	6×10^{-14}	3×10^{-13}
Model 2	1×10^{-13}	3×10^{-12}
Model 3	3×10^{-13}	1.5×10^{-11}

Note: all models use a value for $k_O = 1.5\times10^{-11}$ cm^3 s^{-1}.

For the vibrational deactivation rate, $k_{v,v-1}$, Degen (1972) used the theory of Schwartz and Herzfeld (1954) (SSH). In this theory the vibrational deactivation coefficients are expressed as

$$k_{v,v-1} = (P_{v,v-1}/P_{1,0})k_{1,0}, \quad (2)$$

where $k_{1,0}$ is a constant and the term in parentheses is a scaling factor which represents the ratio of the SSH collision probabilities. For an anharmonic potential well, as with the $A^3\Sigma_u^+$, this scaling factor increases with v' in a non-linear fashion. Concerning the Herzberg emission, a major uncertainty lies in the value of $k_{1,0}$.

We have calculated vibrational distributions for the $A^3\Sigma_u^+$ state using three different sets of values for k_E and $k_{1,0}$. These models are summarized in Table 1. Model 1 uses the low quenching values of Kenner and Ogryzlo while Model 3 uses the high values proposed by Murtagh *et al.* (1986) from the ETON observations. [Our absolute numbers are higher because we have adopted a higher *A*-value—see Bates (1989).] Model 2 uses an intermediate quenching value. As discussed earlier (Murtagh *et al.*, 1986; McDade *et al.*, 1982, 1984), the value of $k_{1,0}$ must also increase as k_E is increased in order that the distribution remains centered about $v' = 5$. In this manner, and taking into account the observed shift with altitude of the

spectrum, one might hope to "tune" the values of $k_{1,0}$ and k_E to produce the best agreement with the data.

The values for k_E in Table 1 assume that O_2 is the dominant electronic quencher rather than N_2. Since both molecules have almost identical scale heights, their effects on the altitude profile are indistinguishable; however, Kenner and Ogryzlo (1983) do indicate that k_{N_2} is about 20 times less than k_{O_2}. For atmospheric composition ratios, this means that N_2 quenching will be less important than O_2 quenching. We have also used a value for atomic oxygen quenching of 1.5×10^{-11} cm^3 s^{-1} which is essentially the laboratory value. For atmospheric composition ratios, this effectively eliminates atomic oxygen as a quencher. This has been supported by all the rocket studies cited previously. We found that without significant O quenching our results were relatively insensitive to the shape of the adopted [O] profile. In order to confirm this we repeated the vibrational calculations using two different O profiles: one from the MSIS86 empirical model (Hedin, 1987) which had a well-defined peak at 98 km, the other derived from our 7620 Å photometer measurement, using the parameterization of McDade *et al.* (1986), which showed a broad peak from 92 to 99 km. Little difference in the calculated vibrational distribution was seen between the two O profiles and thus the absence of a simultaneous O measurement should not affect our conclusions. Of course the magnitude and shape of the calculated Herzberg volume emission rate profile is sensitive to the choice of O; because O was not directly measured, we will not perform such an analysis here. The resulting vibrational distributions from the three models in Table 1 are compared with the data in Figs 5–7.

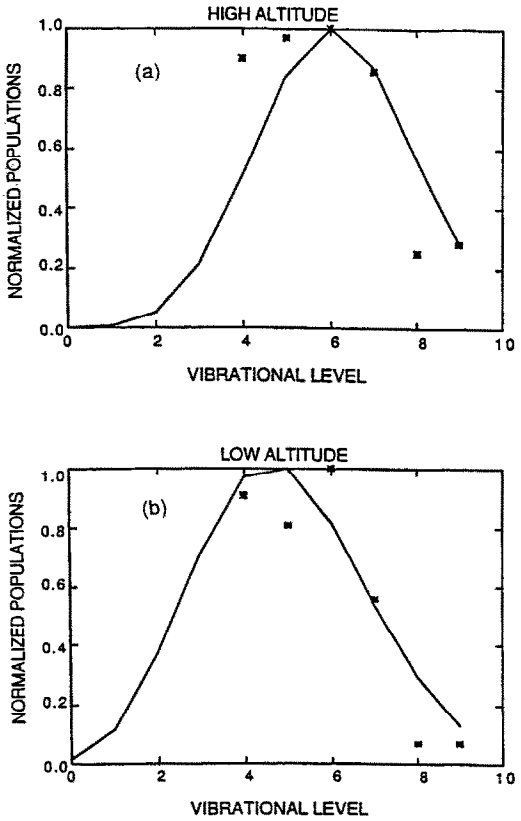

FIG. 5. CALCULATED HERZBERG I VIBRATIONAL DISTRIBUTION AND COMPARISON WITH DATA FOR MODEL 1 (LOW QUENCHING). The values for k_{10} and k_{O_2} are 6×10^{-14} and 3×10^{-13} cm^3 s^{-1} respectively (see text and Table 1). Panel (a) is for the high altitude data. Panel (b) is for the low altitude data.

In Fig. 5 (low quenching—Model 1), the predominant loss of $A^3\Sigma_u^+$ is radiative and a large shift in the vibrational population from high altitude (Fig. 5a) to low altitude (Fig. 5b) is indicated. In this case, the predicted shift is greater than is seen in the data. For example, the contribution from the $v' = 4$ level is predicted to change by a factor of 2 and this is not seen in the data. This agrees with the earlier photometric studies (Murtagh *et al.*, 1986; Kita *et al.*, 1988) which showed that the model of McDade *et al.* (1982) overestimates the vibrational shift when electronic quenching is low. In accordance with the suggestion of McDade and Llewellyn (1986) and Murtagh *et al.* (1986), the magnitude of the shift will be reduced if the electronic quenching is increased. Somewhat improved fits to the data are shown in Fig. 6 (intermediate quenching—Model 2) and Fig. 7 (high quenching—Model 3). In both these figures, the change in the levels with $v' \geqslant 7$ is more approximately matched without a concomitant overestimate of the $v' = 4$ changes, although it does appear that the calculation in Fig. 7 somewhat underestimates the change in population. Unfortunately, neither figure reproduces the exact shape of the vibrational distribution and thus while our results are consistent with enhanced electronic quenching, we cannot constrain our derived quenching value any more closely than the range defined by Figs 6 and 7 (i.e. $Q_{O_2} = 3$–15×10^{-12} cm^3 s^{-1}). In either case, however, our results are consistent with enhanced quenching of the Herzberg emission.

It might be argued here that the uncertainty in placing the airglow layer on an absolute altitude scale would weaken our conclusion. For example, if the layer were much lower than indicated in Fig. 1, the atmospheric densities would be higher and a small

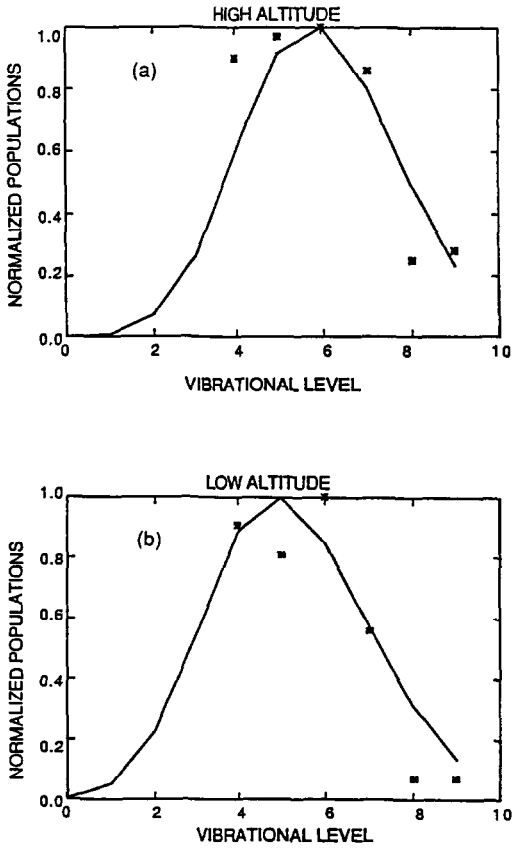

FIG. 6. SAME AS FIG. 5 EXCEPT USING MODEL 2 (INTERMEDIATE QUENCHING).
The values for k_{10} and k_{O_2} are 1×10^{-13} and 3×10^{-12} cm^3 s^{-1}.

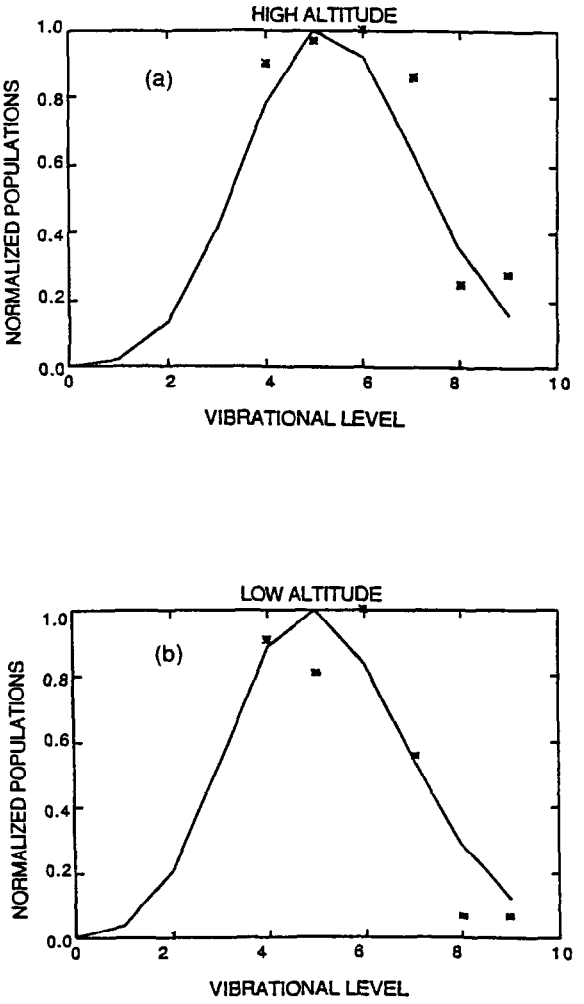

FIG. 7. SAME AS FIG. 5 EXCEPT USING MODEL 3 (HIGH QUENCHING).
The values for k_{10} and k_{O_2} are 3×10^{-13} and 1.5×10^{-11} cm^3 s^{-1}.

amount of vibrational relaxation could still be consistent with the low laboratory values of Kenner and Ogryzlo (1983, 1980). However, in order for our deduced quenching from Model 2 to be as low as 1×10^{-12} cm^3 s^{-1} (still more than twice the Kenner and Ogryzlo value), the background atmosphere would have to be 3 times denser than in our model. This factor of three translates into a 6–7 km altitude shift. This would imply a layer that peaked at 87–88 km which, while not impossible, is highly unlikely and has never been seen. At the other extreme, our value from Model 3 is almost 10 times less than Slanger *et al.*'s (1984) value for $v' = 8$ (adjusted for the 60% difference in A-value). This can only be reconciled if our layer were 12–14 km higher than given in Fig. 1 which, again, is not likely. Thus our uncertainty in the absolute altitude scale is less than the uncertainty in fitting the vibrational distribution.

DISCUSSION

Our analysis lends support to a key prediction of the Degen/McDade theory of vibrational relaxation of O_2 ($A^3\Sigma_u^+$), namely, that the vibrational distribution of the Herzberg I nightglow is altitude dependent. This further strengthens the argument, made most recently by Stegman and Murtagh (1988), that the O_2 A-state is formed by direct recombination of O, rather than through the quenching of a precursor. Our model of the spectrum reveals areas of both agreement and disagreement with previous work. Our results agree with those of Murtagh *et al.* (1986) and

Kita *et al.* (1988) in that the use of the Kenner and Ogryzlo quenching values leads to an overestimate of the amount of change in the vibrational distribution. With increased quenching, the vibrational shift is reduced to the point where, depending upon the exact value chosen, the change in the spectrum may be undetectable using traditional wide band photometers. The need for increased quenching is also consistent with previously published rocket photometer data.

We see two remaining difficulties. First, our results cannot explain the inversion in the altitude variation of the vibrational distribution seen by Murtagh *et al.* (1986) in the ETON data. One possible explanation has been offered by McDade (private communication, 1989). He notes that the signal in the long wavelength photometer used in the ETON experiment appears to increase slightly as the airglow layer is approached from below (see Fig. 4 of Murtagh *et al.*, 1986). This is inconsistent with what one would expect from an extended source but could indicate a contamination from a transient rocket-induced glow. Such contamination, if present, would distort the recovered airglow volume emission profile.

An additional problem is that all of our calculated vibrational distributions showed discrepancies when compared with the observations. As a result, we could not arrive at a "best fit" value for the quenching rate. The problem seems to be that the vibrational relaxation theory as implemented by us leads to smoothly-varying vibrational distributions while the data show significant deviations from a smooth bell-shaped curve. From the data presented here, it is not clear whether the problem lies in an inadequate spectroscopic model or in a neglect of some unknown process. Recently reported ground-based spectra by Stegman *et al.* (1989) as well as other data we have obtained (Sharp and Siskind, 1990, unpublished data) indicate that non-bell-shaped distributions are common. This suggests complications to the simple quenching scheme outlined here. A number of possibilities have been suggested by Murtagh *et al.* (1986) and Slanger and Cosby (1988); for example, cross-relaxation between vibrational levels of different O_2 states as well as multi-quantum deactivation.

Further progress in this area will probably depend upon improved laboratory studies which more realistically simulate the conditions present in the nightglow. For example, in the Kenner and Ogryzlo experiments, vibrational levels greater than $v' = 4$ were not observed in contrast to the nightglow distribution which peaks at $v' = 4$–6. This may reflect a different excitation mechanism in the laboratory which could affect the deduced rate coefficients. Thus, Sharpless *et al.* (1989) have recently concluded that in surface-catalyzed oxygen recombination (e.g. the Kenner and Ogryzlo experiments), the spectral distribution is governed by the behavior of a precursor which they argue is highly vibrationally-excited ground state O_2. The only laboratory spectrum which resembles the nightglow appears to be that of McNeal and Durana (1969); unfortunately they did not perform a detailed vibrational analysis of their data.

SUMMARY

We have searched for an altitude variation in the nightglow spectra from 2670 to 3040 Å obtained by a limb scanning u.v. spectrometer. The evidence suggests that vibrational levels of O_2 ($A^3\Sigma_u^+$) greater than six are depleted at lower altitudes, consistent with a theory of single-step vibrational relaxation. Our model of the data suggests that rapid electronic quenching of O_2 ($A^3\Sigma_u^+$) competes with vibrational relaxation and acts to reduce the change in the spectrum. For quenching by molecular oxygen, a lower limit on the quenching rate is 3×10^{-12} cm^3 s^{-1}. This is consistent with previous rocket observations of the Herzberg nightglow but disagrees with several laboratory measurements of the Herzberg I quenching rate.

Acknowledgements—We acknowledge many enlightening conversations with I. C. McDade. This research was supported by NASA grant NGR23-005-360.

REFERENCES

Bates, D. R. (1989) Oxygen band system transition arrays. *Planet. Space Sci.* **37**, 881.

Broida, H. P. and Gaydon, A. G. (1954) The Herzberg bands of O_2 in an oxygen afterglow and in the night-sky spectrum. *Proc. R. Soc. Lond.* **A222**, 181.

Chamberlain, R. W. (1955) The ultraviolet airglow spectrum. *Astrophys. J.* **121**, 277.

Chamberlain, R. W. (1958) The blue airglow spectrum. *Astrophys. J.* **128**, 713.

Degen, V. (1969) Vibrational populations of O_2 ($A^3\Sigma_u^+$) and synthetic spectra of the Herzberg bands in the nightglow. *J. geophys. Res.* **74**, 5145.

Degen, V. (1972) Excitation of the Herzberg bands of O_2 in laboratory afterglow and night airglow. *J. geophys. Res.* **77**, 6213.

Dufay, J. (1941) Une intepretation possible de certaines radiaions intenses du ciel nocturne dans la region ultraviolette. *C.r. Acad. Sci. Paris* **213**, 284.

Greer, R. G. H., Murtagh, D. P., McDade, I. C., Dickinson, P. H. G., Thomas, L., Jenkins, D. B.,Stegman, J., Llewellyn, E. J., Witt, G., Mackinnon, D. J. and Williams, E. R. (1986) ETON 1: a data base pertinent to the study of

energy transfer in the oxygen nightglow. *Planet. Space Sci.* **34**, 771.

Hedin, A. E. (1987) MSIS-86 Thermospheric Model. *J. geophys. Res.* **92**, 4649.

Hennes, J. P. (1966) Measurement of the ultraviolet nightglow spectrum. *J. geophys. Res.* **71**, 763.

Kenner, R. D. and Ogryzlo, E. A. (1980) Deactivation of O_2 ($A^3\Sigma_u^+$) by O_2, O, and Ar. *Int. J. Chem. Kinetics* **12**, 501.

Kenner, R. D. and Ogryzlo, E. A. (1983) Rate constant for the deactivation of O_2 ($A^3\Sigma_u^+$) by N_2. *Chem. Phys. Lett.* **103**, 209.

Kenner, R. D. and Ogryzlo, E. A. (1984) Quenching of O_2 ($A_{v=2} \rightarrow X_{v=5}$) Herzberg I band by O_2 (*a*) and O. *Can. J. Phys.* **62**, 1599.

Kita, K., Iwagami, N., Ogawa, T., Miyashita, A. and Tanabe, H. (1988) Height distributions of the night airglow emissions in the O_2 Herzberg I system and oxygen green line from a simultaneous rocket observation. *J. Geomagn. Geoelect.* **40**, 1067.

McDade, I. C. and Llewellyn, E. J. (1986) The excitation of O(^{1}S) and O_2 bands in the nightglow: a brief review and preview. *Can. J. Phys.* **64**, 1626.

McDade, I. C., Llewellyn, E. J., Greer, R. G. H. and Murtagh, D. P. (1982) The altitude dependence of the O_2 ($A^3\Sigma_u^+$) vibrational distribution in the terrestrial nightglow. *Planet. Space Sci.* **30**, 1133.

McDade, I. C., Llewellyn, E. J., Greer, R. G. H. and Witt, G. (1984) Altitude dependence of the vibrational distribution of O_2 ($c^1\Sigma_u^-$) in the nightglow and the possible effects of vibrational excitation in the formation of O(^{1}S). *Can. J. Phys.* **62**, 780.

McDade, I. C., Murtagh, D. P., Greer, R. G. H., Dickinson, P. H. G., Witt, G., Stegman, J., Llewellyn, E. J., Thomas, L. and Jenkins, D. B. (1986) ETON 2: quenching parameters for the proposed precursors of O_2 ($b^1\Sigma_g^+$) and O(^{1}S) in the terrestrial nightglow. *Planet. Space Sci.* **34**, 789.

McNeal, R. J. and Durana, C. (1969) Absolute chemiluminescent reaction rates for emission of the O_2 Herzberg bands in oxygen and oxygen-inert-gas afterglows. *J. chem. Phys.* **51**, 2955.

Murtagh, D. P., McDade, I. C., Greer, R. G. H., Stegman, J., Witt, G. and Llewellyn, E. J. (1986) ETON 4: an experimental investigation of the altitude dependence of the O_2 ($A^3\Sigma_u^+$) vibrational populations in the nightglow. *Planet. Space Sci.* **34**, 811.

Schwartz, R. N. and Herzfeld, K. F. (1954) Vibrational relaxation times in gases (three-dimensional treatment). *J. chem. Phys.* **22**, 767.

Sharp, W. E. and Siskind, D. E. (1989) Atomic emission in the ultraviolet nightglow. *Geophys. Res. Lett.* **16**, 1453.

Sharpless, R. L., Jusinski, L. E. and Slanger, T. G. (1989) Surface chemistry of metastable oxygen. 1. Production and loss of the 4–5 eV states. *J. chem. Phys.* **91**, 7936.

Slanger, T. G., Bishel, W. K. and Dyer, M. J. (1984) Photoexcitation of O_2 at 249.3 nm. *Chem. Phys. Lett.* **108**, 472.

Slanger, T. G. and Cosby, P. C. (1988) O_2 spectroscopy below 5.1 eV. *J. phys. Chem.* **92**, 267.

Slanger, T. G. and Huestis, D. L. (1981) O_2 ($c^1\Sigma_u^- - X^3\Sigma_g^-$) emission in the terrestrial nightglow. *J. geophys. Res.* **86**, 3551.

Slanger, T. G. and Huestis, D. L. (1983) The rotationally resolved 3400 to 3800 Å terrestrial nightglow. *J. geophys. Res.* **88**, 4137.

Stegman, J. and Murtagh, D. P. (1988) High resolution spectroscopy of oxygen u.v. airglow. *Planet. Space Sci.* **36**, 927.

Stegman, J., Murtagh, D. P. and Witt, G. (1989) Spectral composition of the O_2 u.v. nightglow. *Trans. Am. geophys. Un. EOS* **70**, 1238.

Swenson, G. R., Mende, S. B. and Llewellyn, E. J. (1989) Imaging observations of lower thermospheric O(^{1}S) and O_2 airglow emissions from *STS* 9: implications of height variations. *J. geophys. Res.* **94**, 1417.

Thomas, R. J. (1981) Analyses of atomic oxygen, the green line and Herzberg bands in the lower thermosphere. *J. geophys. Res.* **86**, 206.